TRANSNAV
http://www.transnav.eu
the International Journal
on Marine Navigation
and Safety of Sea Transportation
Volume 17
Number 4
December 2023

DOI: 10.12716/1001.17.04.09

Analysis of Known and Construction of New Mathematical Models of Forces on a Ship's Rudder in an Unbounded Flow

O. Kryvyi, M. Miyusov & M. Kryvyi
National University "Odessa Maritime Academy", Odessa, Ukraine

ABSTRACT: The forces arising on the ship's rudder at different angles of attack in an unbounded flow are investigated. The components of the resulting force on the rudder are represented in terms of the rudder lift and drag forces, as well as in terms of the normal and tangential forces on the rudder. The well-known mathematical models of hydrodynamic rudder coefficients are analyzed, and their disadvantages are found. New mathematical models of hydrodynamic coefficients have been obtained, in particular, the coefficients of rudder lift and drag, which take into account the aspect ratio of the rudder, its relative thickness and can be applied to any angle of attack of the flow on the rudder. On specific examples for rudders of the NACA series, the adequacy of the proposed models and their consistency with known experimental studies are illustrated. It is shown how the rudder lift and drag change, as well as the components of the resulting force for the maximum possible range of changes in the local drift angle and the rudder angle.

1 INTRODUCTION

The availability of adequate mathematical models of the propulsive ship complex is of crucial importance in the development of effective ship control systems, the construction of high-quality simulators, and in the study of the ship's behavior during maneuvering. Many works are devoted to the construction and application of mathematical models of the propulsive ship complex [1 - 23].

One of the important components of the non-inertial forces and moments acting on the ship are the forces and moments caused by the operation of the ship's rudders, the study of which, in particular, is devoted to works [24 - 31]. The study of the operation of ship rudders is based on the processing of experimental data of model and field tests [2, 3, 25, 26, 28, 29]. Recently, due to the rapid development of Computational Fluid Dynamics (CFD) methods, the Reynolds-Averaged Navier-Stokes (RANS) method has been widely used to solve this problem [27, 30, 31]. Both approaches complement each other and are used to determine the distribution of hydrodynamic forces on the rudders, which is the basis for obtaining mathematical models of these forces with their further consideration in the general mathematical models of the ship's propulsive complex. To build mathematical models of ship rudders at the first stage, it is necessary to have adequate mathematical models of hydrodynamic forces and moment on an isolated rudder in an unbounded flow. Mainly, linear approximations of the specified forces are known and widely used [2, 3, 7 - 17], which use only the first hydrodynamic derivative and sufficiently accurately describe their behavior at small angles of attack of the flow on the rudder, but do not take into account, in particular, the tangent component. Presentations of the components of the resulting hydrodynamic force on the rudder are also known [3, 29], which can be used for a wider range of changes in the phase coordinates of the ship's motion, but they require clarification and further development.

The aim of this work is the construction and numerical analysis of adequate mathematical models of forces on ship rudders in an unbounded flow, which would, on the one hand, cover a sufficiently wide range of changes in the local drift angle and the rudder angle, and on the other hand, would be convenient for use in solving various problems of dynamics of the ship's propulsive complex.

2 VESSEL AND RUDDER SPECIFICATIONS

The geometric and technical characteristics of the ship and the rudder will be denoted as follows: L – length of the ship on waterline; B – breadth of the ship on waterline; T – amidships draft, ρ – mass density of sea water, C_b – block coefficient; $W=C_bLBT$ – displacement volume of the ship; $S = LT\sigma_D$ – area of the underwater part of the centerplane of the ship's hull; σ_D – reduced coefficient of the underwater centerplane of the ship. On modern ships, depending on their purpose, different types of rudders are used. On ocean-going ships single rudders are usually used behind single propellers, which are located in the centerplane. The rudders may differ in the type of projection on the centerplane, namely rectangular or trapezoidal; according to the method of fastening: simplex rudder, spade rudder, semi-balanced (semi-spade) rudder; according to the profile shape: NACA, CAHI, NEZ, HSVA, IFS, Wedge, etc. A detailed classification of ship rudders is presented, in particular, in [29, 30]. Let us dwell in detail on those characteristics of ship rudders that are used in the construction of mathematical models of hydrodynamic forces on the rudder. The main characteristics include the area of the rudder blade S_R, that is, the area limited by the contour of the projection of the rudder on the centerplane, as well as the relative area of the rudder blade $\tilde{S}_R = S_R(LT)^{-1}$. For effective control of the ship, depending on the goals, the relative area of the rudder blade should at least satisfy the condition [32]

$$\tilde{S}_R \geq 0.01 + 0.5C_b^2\left(\frac{B}{L}\right)^2. \qquad (1)$$

When constructing mathematical models of hydrodynamic forces and moments, it is important to check the fulfillment of condition (1). For some types of commercial vessels, Table 2.1 [30, p. 24], shows the reference ratios of the rudder area to the lateral underwater area of the ship's hull. The linear geometric characteristics of the ship's rudders include: its height h_R , that is, the greatest distance between the lower and upper edges, as well as the rudder chord b_R , that is, the distance between the leading edge (nose) and its trailing edge (tail). Since the ship's rudder is not rectangular in plan, for example, trapezoidal, then the value: $b_{Rc} = S_R h_R^{-1}$ is used as the average chord.

The relative thickness value $\tilde{t}_R = t_R b_{Rc}^{-1}$ is also used, where t_R the maximum thickness of the rudder blade. Modern ocean-going merchant ships usually use rudder profiles NACA-0012, NACA-0015, NACA-0018, NACA-0020, NACA-0025, which correspond to the parameter values: 0.12; 0.15; 0.18; 0.20; 0.25. The important parameters of the ship's rudder also include the aspect ratio of the rudder $\Lambda_R = h_R^2 S_R^{-1} = h_R b_{Rc}^{-1}$, which shows how many times the height is greater (or less) than the chord. For marine merchant ships this figure is $1.5 \div 3$, for inland navigation vessels - $0.5 \div 2.0$. Table 1 lists the main technical characteristics of hulls and ship rudders for some types of ocean-going merchant ships.

Table 1. Technical parameters of ships and rudders

Ship	KCS, Container ship	KVLCC2, Tanker	VLGC, Tanker	LPG, Tanker
№	1	2	3	4
L [m]	230	320	226	147
B [m]	32.2	58	36.6	25.5
T [m]	10.8	20,8	11.8	8.8
C_B	0.65	0,81	0.72	0.74
h_R	9.9	14.32	9.65	6.7
b_{Rc}	5.5	7.84	4.76	2.87
$\tilde{S}_R$	0.018	0.01687	0.017	0.01484
Λ_R	1.8	1.827	2.027	2.34
S_R	54.45	115.04	45.934	19.2

An important parameter of the operation of the ship's rudder is also the rudder angle δ, that is the angle of deviation of the rudder from the centerplane of the vessel. The rudder angle is usually considered positive if it is placed counterclockwise from the centerplane. The maximum value of this angle is limited by the design features of the vessel and, usually, for merchant vessels $|\delta_{\max}| = 35^\circ$. This should be taken into account when mathematically modeling the operation of ship's rudders. The operation of the ship's rudder is also affected by the value of the dimensionless Reynolds number on the rudder: $\mathrm{Re} = v_R b_{Rc} \mu^{-1}$, where v_R – the value of the flow velocity on the rudder, μ – the kinematic viscosity of the sea water. Based on the definition of the number Re, its value for each specific vessel depends on the speed of the vessel and is in the range $2 \cdot 10^5 \div 10^7$.

3 HYDRODYNAMIC FORCES ON AN ISOLATED RUDDER IN AN UNBOUNDED FLOW

Consider the hydrodynamic forces on an isolated rudder in an unbounded flow, that is, on a rudder that is not affected by the ship's hull and the propeller. To study the hydrodynamic forces on such rudder, let's introduce the left Cartesian coordinate system $DX_*Y_*Z_*$ (Fig. 1), where D the point of action of the resultant hydrodynamic force $\vec{P}_{R_*}$ on the rudder, and the axis Z_* is directed perpendicularly upwards to the horizontal section of the rudder. The resultant force on the rudder $\vec{P}_{R_*}$ arises due to shifting the rudder to an angle δ and flow on the rudder with a velocity $\vec{v}_R$ at an angle β_R to the axis X_*. In the introduced coordinate system, the angle β_R, which can be considered the local angle of drift on the rudder, and the rudder angle δ, will be positive if viewed counterclockwise. The angle of attack on the rudder is called the angle between the chord of the rudder and the direction of flow on the rudder, i.e. the difference between the rudder angle and the local drift angle (Fig. 1):

$$\alpha_R = \delta - \beta_R . \tag{2}$$

If the angle of attack α_R is positive, then the deviation of the rudder chord from the line of the flow occurs counterclockwise, in the opposite case, clockwise. In the flat Cartesian coordinate system, the resultant force on the rudder allows expression

$$\vec{P}_{R_*} = \vec{P}_{Y_*} + \vec{P}_{X_*} = P_X\vec{i} + P_Y\vec{j} , \tag{3}$$

where $\vec{i}$ and $\vec{j}$ are the unit vectors in the given coordinate system. The values of the longitudinal P_X and transverse P_Y components of the resulting force on the rudder are to be determined. Specifically, these components are taken into account in the general mathematical models of the dynamics of the ship's propulsion complex. Usually, the components P_X and P_Y are represented in terms of the magnitude of the lift and the drag on the rudder, or the magnitude of the normal force P_N and the tangential force P_S on the rudder. Let's establish a connection between the indicated parameters, for this we consider two more Cartesian coordinate systems associated with the rudder: L_*DD_* and N_*DS_*. The first of these systems is formed by turning the system X_*DY_* through an angle β_R, the second - by turning it through an angle δ counterclockwise (see Fig. 1).

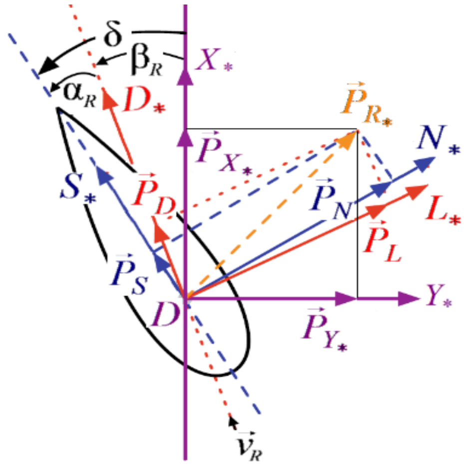

Figure 1. Forces on an isolated rudder

The resultant force $\vec{P}_{R_*}$ in the created coordinate systems allows the following expressions:

– in the coordinate system L_*DD_*:

$$\vec{P}_{R_*} = \vec{P}_L + \vec{P}_D = P_L\vec{i} + P_D\vec{j} , \tag{4}$$

– in the coordinate system N_*DS_*

$$\vec{P}_{R_*} = \vec{P}_N + \vec{P}_S = P_N\vec{i} + P_S\vec{j} . \tag{5}$$

In formulas (4) - (5) $\vec{i}$ and $\vec{j}$ are the unit vectors in the corresponding coordinate system. Representations (3) – (5) and the transformation formulas when the coordinate axes are rotated make it possible to express the values of the longitudinal and transverse components of the resultant force $\vec{P}_{R_*}$ through the components (P_L, P_D) and (P_N, P_S):

$$\begin{cases} P_X = \sin\beta_R \cdot P_L + \cos\beta_R \cdot P_D \\ P_Y = \cos\beta_R \cdot P_L - \sin\beta_R \cdot P_D \end{cases} , \tag{6}$$

$$\begin{cases} P_X = \sin\delta \cdot P_N + \cos\delta \cdot P_S \\ P_Y = \cos\delta \cdot P_N - \sin\delta \cdot P_S \end{cases} . \tag{7}$$

It is not difficult to establish the following relationship between the components (P_L, P_D) and (P_N, P_S):

$$\begin{cases} P_D = \sin\alpha_R \cdot P_N + \cos\alpha_R \cdot P_S \\ P_L = \cos\alpha_R \cdot P_N - \sin\alpha_R \cdot P_S \end{cases} . \tag{8}$$

When studying hydrodynamic forces on a ship's rudder, dimensionless hydrodynamic coefficients of transverse and longitudinal forces, lift and drag, as well as normal and tangential forces on the ship's rudder are usually introduced:

$$C^*_{YR} = \frac{2P_Y}{\rho v_R^2 S_R},\ C^*_{XR} = \frac{2P_X}{\rho v_R^2 S_R},\ C_{LR} = \frac{2P_L}{\rho v_R^2 S_R}$$
$$C_{DR} = \frac{2P_D}{\rho v_R^2 S_R},\ C_{NR} = \frac{2P_N}{\rho v_R^2 S_R},\ C_{SR} = \frac{2P_S}{\rho v_R^2 S_R} \tag{9}$$

At the same time, the dimensionless coefficient of the resultant force can be expressed as follows

$$C_R = \frac{|\vec{P}_{R*}|}{\rho v_R^2 S_R} = \sqrt{(C^*_{YR})^2 + (C^*_{XR})^2} = \sqrt{C^2_{LR} + C^2_{DR}} = \sqrt{C^2_{NR} + C^2_{SR}}. \tag{10}$$

Taking into account representations (9), relations (6) - (8) will be rewritten as follows

$$\begin{cases} C^*_{XR} = \sin\beta_R \cdot C_{LR} + \cos\beta_R \cdot C_{DR} \\ C^*_{YR} = \cos\beta_R \cdot C_{LR} - \sin\beta_R \cdot C_{DR} \end{cases}, \tag{11}$$

$$\begin{cases} C^*_{XR} = \sin\delta \cdot C_{NR} + \cos\delta \cdot C_{SR} \\ C^*_{YR} = \cos\delta \cdot C_{NR} - \sin\delta \cdot C_{SR} \end{cases}. \tag{12}$$

$$\begin{cases} C_{DR} = \sin\alpha_R \cdot C_{NR} + \cos\alpha_R \cdot C_{SR} \\ C_{LR} = \cos\alpha_R \cdot C_{NR} - \sin\alpha_R \cdot C_{SR} \end{cases}. \tag{13}$$

The ratio $k_L = P_L / P_D = C_{LR} / C_{DR}$ is called the coefficient of hydrodynamic quality of the rudder blade [2, 3], and the inverse value $k_D = 1/k_L$ is called the coefficient of the inverse quality of the rudder blade. We will also introduce the coefficient of tangential force $k_S = C_{SR}/C_{NR}$, which determines the effect of the tangential component of the force on the rudder. The coefficients k_L, k_D and k_S are functions of the aspect ratio of the rudder blade. Let's establish the relationship between the coefficients k_L, k_D and k_S, for this, by dividing the second equality in (13) by the first, we get

$$k_L = \frac{\cos\alpha_R - k_S \sin\alpha_R}{\sin\alpha_R + k_S \cos\alpha_R}, \tag{14}$$

From here we get the following representation

$$k_S = \frac{\cos\alpha_R - k_L \sin\alpha_R}{\sin\alpha_R + k_L \cos\alpha_R}. \tag{15}$$

Denote by $\operatorname{tg}\varphi_D = k_L$, $\operatorname{tg}\varphi_N = k_S$, where φ_D, φ_N respectively, the angles between vectors $\vec{P}_D$, $\vec{P}_N$ and the resulting vector $\vec{P}_{R_*}$, then from relations (14), (15), we obtain the representation

$$k_L = -\operatorname{ctg}(\alpha_R + \varphi_N),\quad k_S = -\operatorname{ctg}(\alpha_R + \varphi_D). \tag{16}$$

Coefficients k_L, k_D and k_S make it possible to represent expressions (11), (12) and (13) as

$$\begin{cases} C^*_{XR} = C_{LR} \cdot (\sin\beta_R + k_D \cos\beta_R) \\ C^*_{YR} = C_{LR} \cdot (\cos\beta_R - k_D \sin\beta_R) \end{cases}; \tag{17}$$

$$\begin{cases} C^*_{XR} = C_{NR} \cdot (\sin\delta + k_D \cos\delta) \\ C^*_{YR} = C_{NR} \cdot (\cos\delta - k_D \sin\delta) \end{cases}; \tag{18}$$

$$\begin{cases} C^*_{DR} = C_{NR} \cdot (\sin\alpha_R + k_D \cos\alpha_R) \\ C^*_{LR} = C_{NR} \cdot (\cos\alpha_R - k_D \sin\alpha_R) \end{cases}. \tag{19}$$

According to Figure 1, the angle between the vector of the resultant hydrodynamic force $\vec{P}_{R_*}$ and the vector $\vec{P}_{Y_*}$ is equal to the sum of the rudder angle δ and the angle φ_N. This makes it possible to represent the dimensionless coefficients of the transverse and longitudinal forces of the rudder through the dimensionless coefficient of the resulting force C_R:

$$\begin{cases} C^*_{XR} = C_R \sin(\delta + \varphi_N) \\ C^*_{YR} = C_R \cos(\delta + \varphi_N) \end{cases}. \tag{20}$$

When building a general mathematical model of the ship's propulsive complex, dimensionless hydrodynamic coefficients of the transverse and longitudinal forces C^*_{YR} and C^*_{XR} on the rudder are used. To determine them, you can use the following three approaches:

1. use representations (11) or (17), if mathematical models for rudder lift coefficient C_{LR} and drag coefficient C_{DR} are known (or instead of C_{DR}, coefficient of inverse quality of the rudder k_D);
2. use representations (12) or (18), if mathematical models for the coefficients of normal force C_{NR} and tangential force C_{SR} on the rudder are known (or instead of C_{SR}, coefficient of tangential force k_S);
3. use representations (20), if mathematical models for (P_L, P_D) or for (P_N, P_S) are known.

4 ANALYSIS OF EXISTING MATHEMATICAL MODELS OF HYDRODYNAMIC COEFFICIENTS ON THE RUDDER

When building mathematical models of ship rudders, it is important to know the critical value of the angle of attack on the rudder α_{Rk}, i.e., the angle of attack at which the stall occurs on the rudder blade and its lift is sharply reduced. The set of values of angles of attack $|\alpha_R| \le \alpha_{Rk}$ is called pre-critical, and the set of values $|\alpha_R| > \alpha_{Rk}$ is called supercritical. The angles $\pm\alpha_{Rk}$ are actually the angles of the maximum value of the rudder lift coefficient C_{LR}, while the angle of maximum efficiency has a slightly smaller value, due to the increase in the rudder drag coefficient C_{DR}. It should also be noted that the value of the angle α_{Rk} for the rudder located in the propeller slipstream increases on average by $15^\circ \div 20^\circ$. The angle α_{Rk} depends on the technical characteristics of the rudder, in particular its aspect ratio, to determine its values using experimental data [2, 3], we obtain table 2.

Table 2. Dependence of the critical value of the angle of attack α_{Rk} [deg] from the aspect ratio Λ_R

Λ_R	0.5	0.75	1	1.25	1.5	2	3	5
α_{Rk}	45.5	41	36	30.5	25.5	23.75	19.5	16.7

Based on these data, with the help of regression analysis, we will get the following representation

$$\alpha_{Rk} = 29.6824 \cdot \Lambda_R^{-0.356}. \tag{21}$$

Experimental studies [2, 3, 26] show that the rudder lift coefficient C_{LR} and the rudder drag coefficient C_{DR} depends to varying degrees on the shape, thickness of the rudder, Reynolds number, but most of all on the rudder aspect ratio Λ_R and the angle of attack of the flow on the rudder α_R. In particular, for small to critical angles of attack, a linear approximation of the lift coefficient is used, i.e., a Taylor series expansion along the angle of attack:

$$C_{LR}(\alpha_R) = f(\alpha_R) = \sum_{j=0}^{\infty} \frac{f^{(j)}(0)}{j!} \cdot \alpha_R^j = f(0) + f'(0) \cdot \alpha_R + o(\alpha_R).$$

In this case, only the second term is used. The first is equal to zero: $f(0) = C_{LR}(0) = 0$, due to physical considerations, therefore

$$C_{LR} = C'_{LR} \cdot \alpha_R. \tag{22}$$

To designate the hydrodynamic derivative $C'_{LR} = \left.\frac{dC_{LR}}{d\alpha_R}\right|_{\alpha_R=0}$, one can use the formula [2, 3]:

$$C'_{LR} = \frac{2\pi\Lambda_R}{2 + \sqrt{\Lambda_R^2 + 4}}, \tag{23}$$

or Prandtl's improved formula

$$C'_{LR} = \frac{2\pi\kappa_0\Lambda_R}{2 + \Lambda_R}, \tag{24}$$

where $\tilde{C}_d = 2$ is the coefficient for spade and semi-spade rudders of marine vessels.

For a wider range of the angle of attack, the following formula is known [2]

$$C_{LR} = C'_{LR} \cdot \sin\alpha_R + \tilde{C}_d \sin^2\alpha_R \cdot \cos\alpha_R, \tag{25}$$

where $\tilde{C}_d = 2$ for conventional rudders and $\tilde{C}_d = 1.2 \div 1.5$ for rudders with rounded side projections.

The following formula can be used for the rudder drag coefficient [3]:

$$C_{DR} = C_{D0} + K_D \cdot \sin^2\alpha_R + \tilde{C}_d \cdot \sin^3\alpha_R, \tag{26}$$

where $C_{D0} = (0.0221 - 0.0023\lg\mathrm{Re})\tilde{C}$. The coefficients $\tilde{C} = \tilde{C}(\tilde{t}_R)$ and $K_D(\Lambda_R)$ are determined using graphs [3]. Note that at $\alpha_R = 0$, as a rule, the value of the drag force coefficient is chosen approximately: $C_{D0} \approx 0.014$.

There are also other representations [29] for the lift and drag coefficients of the rudder, also obtained on the basis of experimental data processing:

$$C_{LR} = 2\pi \frac{\Lambda_R(\Lambda_R + 0.7)}{(\Lambda_R + 1.7)^2} \cdot \sin\alpha_R + C_Q \sin\alpha_R \cdot |\sin\alpha_R| \cdot \cos\alpha_R \tag{27}$$

$$C_{DR} = \frac{C_{LD}^2}{\pi \cdot \Lambda_R} + C_Q \cdot |\sin\alpha_R|^3 + C_{D0} \tag{28}$$

$$C_{D0} = 2.5 \frac{0.075}{(\lg\mathrm{Re} - 2)^2}.$$

The authors of the model recommend taking the value of the constant C_Q equal to one: $C_Q = 1$.

Within the framework of the second approach [7, 8], a linear approximation of the normal force coefficient takes place. Under the assumptions of smallness α_R, the dependence is represented not by the angle of attack α_R, but by its sinus $\sin\alpha_R$, i.e.

$$C_{NR} = C'_{NR} \cdot \sin\alpha_R. \tag{29}$$

Empirical representation is used to calculate the hydrodynamic derivative of the normal force:

$$C'_{NR} = \left.\frac{dC_{NR}}{d\alpha_R}\right|_{\alpha_R=0} = \frac{6.13\Lambda_R}{\Lambda_R + 2.25}. \tag{30}$$

It should be noted that in this case the value of the tangential force on the rudder is neglected: $C_{SR} = 0$.

Using the methods of direct numerical modeling RANS [30], representations (22) and (29) are somewhat improved by taking into account the relative thickness of the rudders

$$C_{LR} = \frac{\Lambda_R}{\Lambda_R + 2.25} \cdot (s_L \sin\alpha_R + c_L). \tag{31}$$

$$C_{DR} = \frac{\Lambda_R}{\Lambda_R + 2.25} \cdot (s_D \sin\alpha_R + c_D). \tag{32}$$

$$C_{NR} = \frac{\Lambda_R}{\Lambda_R + 2.25} \cdot (s_N \sin\alpha_R + c_N). \tag{33}$$

The constants in representations (31) - (33), depending on the relative thickness $\tilde{t}_R$, are given in Table 4.2 [30, p. 89] for some types of ship's rudders.

Studies of representations for hydrodynamic coefficients on a ship's rudder have shown significant shortcomings of existing models. In particular, representations (22), (29) and (31) - (32) can be applied only at small to critical drift angles, while representations (31), (33) can be considered more accurate, where the relative thickness of the rudder is taken into account. In representations (25), (26) and (32), the properties of the oddness of the lift coefficient and the parity of the drag coefficient of the rudder are violated, so they cannot be used for negative values of the angle of attack α_R on the rudder. In representations (27) and (28) there are non-differentiable functions, such as $|\sin\alpha_R|$. Therefore, for a general description of the behavior of hydrodynamic coefficients, they are acceptable, but as the right-hand parts of the differential equations of the dynamics of the propulsive complex, their use is incorrect, since in this case the phase coordinates of the ship's motion will be discontinuous functions.

5 CONSTRUCTION AND ANALYSIS OF NEW MATHEMATICAL MODELS OF HYDRODYNAMIC FORCE COEFFICIENTS ON THE RUDDER

To eliminate the indicated shortcomings of the existing mathematical models of hydrodynamic force coefficients on the rudder, we will search for the lift force coefficient as follows

$$C_{LR} = C'_{LR} \cdot \sin\alpha_R - \chi(\Lambda_R) \cdot \sin^3\alpha_R, \tag{34}$$

where $\chi(\Lambda_R)$ the function of the rudder aspect ratio Λ_R is not yet known, which we will determine based on the following considerations. Representation (34) must reach a maximum at critical values of the angle of attack, so the condition must be fulfilled

$$\left.\frac{dC_{LR}}{d\alpha_R}\right|_{\alpha_R=\alpha_{kR}} \equiv C'_{LR} \cdot \cos\alpha_{kR} - 3\chi(\Lambda_R) \cdot \sin^2\alpha_{kR} \cdot \cos\alpha_{kR} = 0. \tag{35}$$

From here

$$\alpha_{kR} = \arcsin\sqrt{\frac{C'_{LR}}{6\chi(\Lambda_R)}}. \tag{36}$$

Equating this expression and representation (21), we find the expression for the unknown function

$$\chi(\Lambda_R) = \frac{C'_{LR}}{3\sin^2(29.6824 \cdot \Lambda_R^{-0.356})} \tag{37}$$

After substituting (37) into (34), we obtain

$$C_{LR} = C'_{LR} \cdot \left(\sin\alpha_R - \frac{\sin^3\alpha_R}{3\sin^2(29.6824 \cdot \Lambda_R^{-0.356})}\right). \tag{38}$$

For the hydrodynamic derivative C'_{LR}, after summarizing expressions (23), (24) and (31), with the help of regression analysis, we obtain the following representation, which depends both on the aspect ratio and on the relative thickness of the rudder:

$$C'_{LR} = \frac{\Lambda_R \cdot \eta_L(\tilde{t}_R)}{2.25 + \Lambda_R}, \tag{39}$$

$$\eta_L(\tilde{t}_R) = -50.503 \cdot (\tilde{t}_R)^2 + 11.123 \cdot \tilde{t}_R + 5.638.$$

Similarly, for the hydrodynamic derivative of the normal force on the rudder, the following representations can be obtained.

$$C'_{NR} = \frac{\Lambda_R \cdot \eta_N(\tilde{t}_R)}{2.25 + \Lambda_R}, \tag{40}$$

$$\eta_N(\tilde{t}_R) = -54.123 \cdot (\tilde{t}_R)^2 + 12.512 \cdot \tilde{t}_R + 5.451.$$

To calculate the hydrodynamic drag coefficient on the rudder, it is proposed to use the following dependences on the powers of the sine of the angle of attack

$$C_{DR} = C_{D0} + K_D \cdot \sin^2\alpha_R + \tilde{C}_d \cdot \sin^4\alpha_R, \tag{41}$$

where $C_{D0} = (0.0221 - 0.0023\lg\mathrm{Re})\tilde{C}$; for the coefficients $\tilde{C} = \tilde{C}(\tilde{t}_R)$ and $K_D(\Lambda_R)$, the following expressions were obtained by regression methods based on experimental data [2, 3].

$$\tilde{C} = 1.36 - 4.09\tilde{t}_R + 29.36\tilde{t}_R^2. \tag{42}$$

$$K_D = 0.856\Lambda_R - 0.188\Lambda_R^2. \tag{43}$$

Figures 2 and 3 show the dependence of the hydrodynamic derivatives C'_{LR}, C'_{NR}, respectively, on the aspect ratio Λ_R at constant values of the relative thickness, and on the relative thickness $\tilde{t}_R$ at constant values of the aspect ratio. In both figures, solid lines show the value of the derivative C'_{LR}, dotted lines show the value of the derivative C'_{NR}.

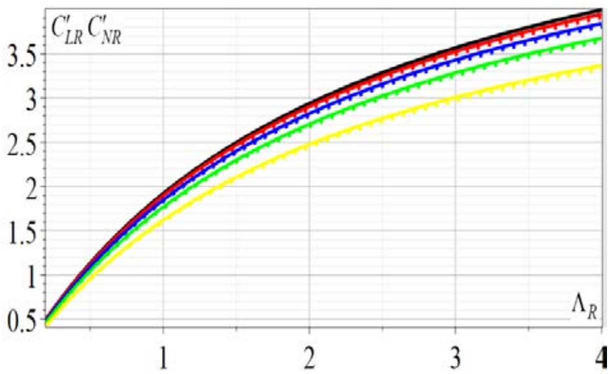

Figure 2. Dependence of derivatives C'_{LR}, C'_{NR} from Λ_R

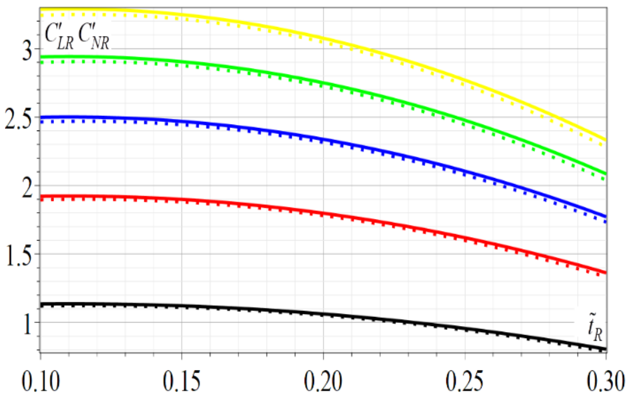

Figure 3. Dependence of derivatives C'_{LR}, C'_{NR} from $\tilde{t}_R$

In fig. 2 black, red, blue, green, and yellow lines are obtained, respectively, at values of $\tilde{t}_R$: 0.12; 0.15; 0.18; 0.21; 0.25. In fig. 3 black, red, blue, green, and yellow lines obtained, respectively, at values of Λ_R 0.5, 1.0; 1.5; 2.0; 2.5. The three-dimensional figure 4 shows the general picture of the change in the behavior of the hydrodynamic derivative C'_{LR}, from the change in the values of the rudder aspect ratio Λ_R and the relative thickness $\tilde{t}_R$. The obtained numerical results confirm the adequacy of the obtained mathematical models (38) and (39), and their consistency with the known results [27, 30].

In particular, it was confirmed that hydrodynamic derivatives C'_{LR} and C'_{NR} do not have significant differences, but they significantly depend on the rudder aspect ratio Λ_R and relative thickness of the rudder $\tilde{t}_R$, which must be taken into account when building mathematical models of hydrodynamic forces caused by the operation of ship rudders. Figure 5 shows the dependences on the angle of attack on the rudder α_R for the lift coefficient C_{LR} obtained using the proposed mathematical model (38) (continuous lines) and using the mathematical model (31) (dotted lines) for the NACA-0020 rudder. At the same time, the black, red, blue, green, and yellow lines are obtained, respectively, at values of the rudder aspect ratio Λ_R of 0.5; 1; 1.5; 2; 2.5.

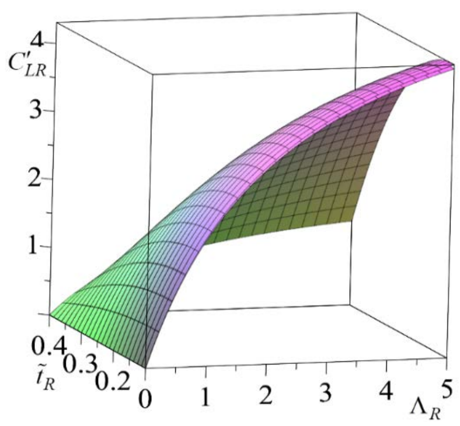

Figure 4. Dependence of the derivative C'_{LR} on Λ_R and $\tilde{t}_R$.

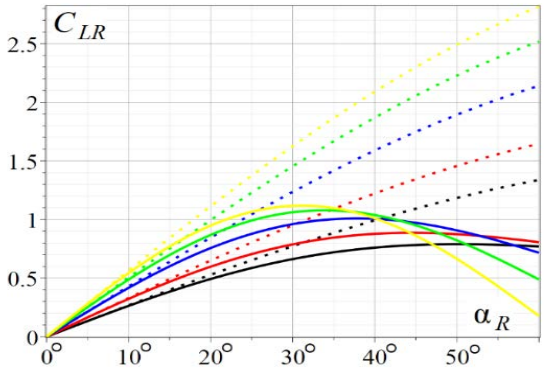

Figure 5. Dependencies C_{LR} on the angle of attack α_R

The given results show that at small values of the angle of attack of the flow on the rudder $|\alpha_R| \le 15^\circ$, both models agree well, but at angles $|\alpha_R| > 15^\circ$, significant differences are observed. According to model (31), the lift coefficient continues to increase with the increase in the angle of attack on the rudder, which does not correspond to the known [2, 3, 25] results of experimental studies. According to the proposed model (38), (39), the coefficient C_{LR} for all rudders reaches a critical value, after which the stall occurs on the rudder and the lift of the rudder decreases. Moreover, the greater the rudder aspect ratio, the smaller the value of the critical angle of attack. These results are fully consistent with the results of known experimental studies.

Figure 6 shows a general picture of the behavior of the lift coefficient C_{LR} depending on the change in the angle of attack α_R on the rudder and the rudder aspect ratio, surface 1 corresponds to the proposed mathematical model (38), (39), surface 2 - model (31).

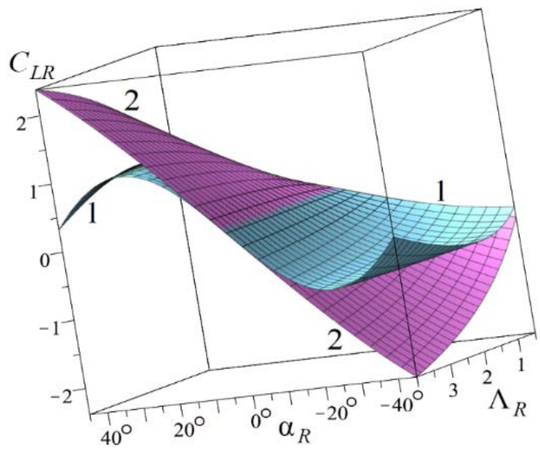

Figure 6. Dependence C_{LR} on α_R and Λ_R.

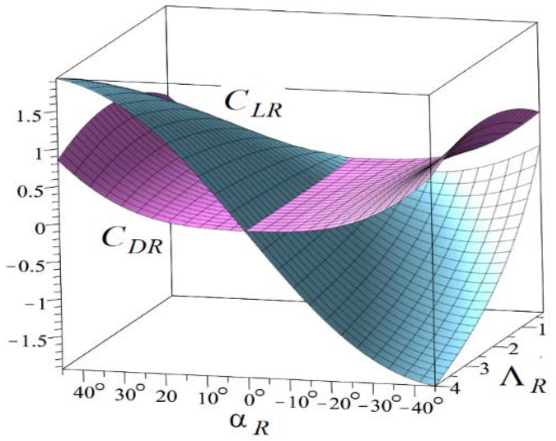

Figure 7. Dependence C_{LR}, C_{DR} on α_R and Λ_R.

Figure 7, using the proposed mathematical models (38), (39) and (40) - (42), shows the dependences of the lift coefficient C_{LR} and the drag coefficient C_{DR} of the rudder on the change in the angle of attack α_R on the NACA-0020 rudder at different values of the rudder aspect ratio Λ_R. Calculations, in particular, show that when the angle of attack increases, the coefficient C_{DR} increases, and when $|\alpha_R| > 15^\circ$ the drag of the rudder becomes commensurate with the lift and it cannot be neglected. It is also noticeable that the drag of the rudder reaches its maximum value at aspect ratios $\Lambda_R \in (1.8; 2.2)$, and the lift increases when the aspect ratio of the rudder increases.

The obtained results are in good agreement with the experimental studies of the lift and the drag of the rudder. Figures 8, 9 show the dependence of the hydrodynamic coefficients, respectively, for the components P_x and P_y the resulting force on the NACA-0020 rudder for a wide range of changes in the local drift angle β_R and the rudder angle δ. The results are obtained using representations (11) and the obtained dependencies (38), (40). At the same time, surface 1 in both figures corresponds to the rudder with aspect ratio $\Lambda_R = 0.5$, surface 2 – with aspect ratio $\Lambda_R = 2$.

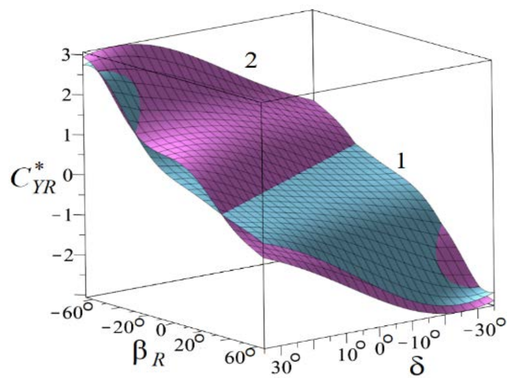

Figure 8. Dependence C^*_{YR} on β_R and δ.

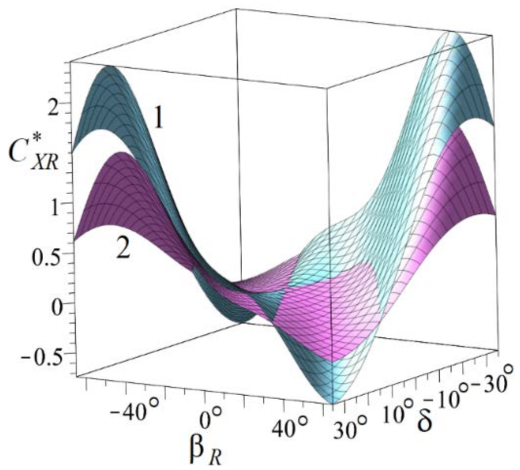

Figure 9. Dependence C^*_{XR} on β_R and δ.

The results of the calculations show the adequacy of the obtained mathematical models of the hydrodynamic coefficients of the resultant force on the rudder for the maximum possible area of change in the local drift angle and the rudder angle. The obtained results make it possible to evaluate the influence of the drift angle β_R and the rudder angle δ on the behavior of the coefficients C^*_{YR} and C^*_{XR}. In particular, the lift and the drag of the rudder are greater if the local drift angle and the rudder angle have different signs than if these angles have the same signs. This means that it is easier to turn the ship in the direction of the ship's drift than in the opposite direction. In addition, the component P_X of the resultant force $\vec{P}_{R_*}$ on the rudder, at drift angles greater than the rudder angle, will have a negative sign, that is, the force $\vec{P}_{X_*}$ acting in the direction of the ship's movement. The dependence of both forces on the rudder aspect ratio is also noticeable.

6 CONCLUSIONS

The existing and proposed new effective and convenient mathematical models for the lift and drag of the rudder in an unbounded flow for a wide range of changes in the local drift angle and the rudder angle and which take into account the rudder thickness and its aspect ratio are analyzed and proposed. On the basis of these models, a numerical analysis of the behavior of the longitudinal and transverse force on the rudder was carried out for the maximum possible range of values of the local drift angle and the rudder angle.

The obtained results will make it possible to build general adequate mathematical models of the ship's propulsion complex, in particular, they are decisive for determining the forces caused by the operation of the ship's rudders, taking into account the influence of the propeller and the ship's hull.

REFERENCES

[1] Pershytz R. Y.: Dynamic control and handling of the ship. L: Sudostroenie, 1983

[2] Sobolev G.C.: Dynamic control of ship and automation of navigation. L.: Sudostroenie, 1976

[3] Gofman A. D.: Propulsion and steering complex and ship maneuvering. Handbook. L .: Sudostroyenie.1988.

[4] Miyusov M. V.: Modes of operation and automation of motor vessel propulsion unit with wind propulsors. Odessa, 1996.

[5] Kryvyi O. F.: Methods of mathematical modeling in navigation. ONMA, Odessa, 2015.

[6] Kryvyi O. F, Miyusov M. V.: Mathematical model of movement of the vessel with auxiliary wind-propulsors, Shipping & Navigation, v. 26, pp.110-119, 2016.

[7] Inoe S., Hirano M., Kijima K.: Hydrodynamic derivatives on ship maneuvering, Int. Shipbuilding Progress, v. 28, № 321, pp. 67-80, 1981.

[8] Kijima K.: Prediction method for ship maneuvering performance in deep and shallow waters. Presented at the Workshop on Modular Maneuvering Models, The Society of Naval Architects and Marine Engineering, v.47, pp.121 130, 1991.

[9] Yasukawa H., Yoshimura Y.: Introduction of MMG standard method for ship manoeuvring predictions, J Mar Sci Technol, v. 20, 37–52pp, 2015. DOI 10.1007/s00773-014-0293-y

[10] Yoshimura Y., Masumoto Y.: Hydrodynamic Database and Manoeuvring Prediction Method with Medium High-Speed Merchant Ships and Fishing, International Conference on Marine Simulation and Ship Maneuverability (MARSIM 2012) pp.494-504.

[11] Yoshimura Y., Kondo M.: Tomofumi Nakano, et al. Equivalent Simple Mathematical Model for the Manoeuvrability of Twin-propeller Ships under the same propeller-rps, Journal of the Japan Society of Naval Architects and Ocean Engineers, v.24, №.0, p.157. 2016, https://doi.org/10.9749/jin.133.28

[12] Wei Zhang, Zao-Jian Zou: Time domain simulations of the wave-induced motions of ships in maneuvering condition, J Mar Sci Technol, 2016, v. 21, pp. 154–166. DOI 10.1007/s00773-015-0340-3

[13] Wei Zhang, Zao-Jian Zou, De-Heng Deng: A study on prediction of ship maneuvering in regular waves, Ocean Engineering, v. 137, pp 367-381, 2017, http://dx.doi.org/10.1016/ j.oceaneng. 2017.03.046

[14] Erhan Aksu, Erkan Köse: Evaluation of Mathematical Models for Tankers' Maneuvering Motions, JEMS Maritime Sci, v.5 №1, pp. 95-109, 2017. DOI: 10.5505/jems.2017.52523

[15] Kang D., Nagarajan V., Hasegawa K. et al: Mathematical model of single-propeller twin-rudder ship, J Mar Sci Technol, v. 13, pp.207–222, 2008, https://doi.org/10.1007/s00773-008-0027-0

[16] Shang H., Zhan C., Z. Liu Z.: Numerical Simulation of Ship Maneuvers through Self-Propulsion, Journal of Marine Science and Engineering, 9(9):1017, 2021. https://doi.org/10.3390/jmse9091017

[17] Shengke Ni., Zhengjiang Liu, and Yao Cai.: Ship Manoeuvrability-Based Simulation for Ship Navigation in Collision Situations, J. Mar. Sci. Eng. 2019, 7, 90; doi:10.3390/jmse7040090

[18] Sutulo S. & C. Soares G.: Mathematical Models for Simulation of Maneuvering Performance of Ships, Marine Technology and Engineering, (Taylor & Francis Group, London), p 661–698, 2011

[19] Kryvyi O. F, Miyusov M. V.: "Mathematical model of hydrodynamic characteristics on the ship's hull for any drift angles", Advances in Marine Navigation and Safety of Sea Transportation. Taylor & Francis Group, London, UK., pp. 111-117, 2019

[20] Kryvyi O. F, Miyusov M. V.: "The Creation of Polynomial Models of Hydrodynamic Forces on the Hull of the Ship with the help of Multi-factor Regression Analysis", 8 International Maritime Science Conference. IMSC 2019. Budva, Montenegro, pp.545-555 http://www. imsc2019. ucg.ac.me/IMSC2019_ BofP. pdf

[21] Kryvyi O., Miyusov M.V.: Construction and Analysis of Mathematical Models of Hydrodynamic Forces and Moment on the Ship's Hull Using Multivariate Regression Analysis, TransNav, the International Journal on Marine Navigation and Safety of Sea Transportation, Vol. 15, No. 4, doi:10.12716/1001.15.04.18, pp. 853-864, 2021

[22] Kryvyi O. F, Miyusov M. V.: Mathematical models of hydrodynamic characteristics of the ship's propulsion complex for any drift angles, Shipping & Navigation, v. 28, pp. 88-102, 2018. DOI: 10.31653/2306-5761.27.2018.88-102

[23] Kryvyi O. F, Miyusov M. V.: New mathematical models of longitudinal hydrodynamic forces on the ship's hull, Shipping & Navigation, v. 30, pp. 88-89, 2020. DOI: 10.31653/2306-5761. 30. 2020.88-98

[24] Kryvyi O. F, Miyusov M. V., Kryvyi M. O.: Mathematical modelling of the operation of ship's propellers with different maneuvering modes, Shipping & Navigation, v. 32, pp. 71-88, 2021. DOI: 10.31653/2306-5761.32.2021.71-88

[25] Molland A.F., Turnock S.R.: Wind tunnel investigation of the influence of propeller loading on ship rudder performance. Technical report, University of Southampton, Southampton, UK, 1991

[26] Molland A.F., Turnock S.R.: Further wind tunnel investigation of the influence of propeller loading on ship rudder performance. Technical report, University of Southampton, Southampton, UK, 1992

[27] Molland A.F., Turnock S.R.: Marine rudders and control surfaces: principles, data, design and applications, 1st edn. Elsevier Butterworth-Heinemann, Oxford, 2007

[28] Ladson CL (1988) Effects of Independent Variation of Mach and Reynolds Numbers on the Low-Speed Aerodynamic Characteristics of the NACA 0012 Airfoil Section. Technical report, Langley Research Center, Hampton, Virginia, USA, 1988

[29] Bertram, V. Practical Ship Hydrodynamic, 2nd ed.; Elsevier Butterworth-Heinemann: Oxford, UK, 2012; p. 284.

[30] Liu J.: Mathematical Modeling of Inland Vessel Maneuverability Considering Rudder Hydrodynamics, 2020. https://doi.org/10.1007/978-3-030-47475-1_4

[31] Shin Y-J, Kim M-C, Kang J-G, Kim J-W. Performance Improvement in a Wavy Twisted Rudder by Alignment of the Wave Peak. Applied Sciences. 2021; 11(20):9634. https://doi.org/10.3390/app11209634 (CDF)

[32] Veritas D.N.: Hull equipment and appendages: stern frames, rudders and steering gears. Rules for Classification of Steel Ships, pp 6–28, part 3, chapter 3, section 2, 2000